Articles

Design, Synthesis, and Evaluation of Conformationally Constrained Tongs, New Inhibitors of HIV-1 Protease Dimerization

Ahmed Bouras,[§] Nicole Boggetto,[⊥] Zohra Benatalah,[§] Eve de Rosny,[⊥] Sames Sicsic,*,[§] and Michèle Reboud-Ravaux[⊥]

BIOCIS, URA-CNRS 1843, Faculté de Pharmacie, Université de Paris-sud, 5 rue J. B. Clément, F-92296 Châtenay-Malabry Cedex, France, and Laboratoire d'Enzymologie Moléculaire et Fonctionnelle, Département de Biologie Supramoléculaire et Cellulaire, Institut Jacques Monod, Universités de Paris VI et VII, 2 place Jussieu, F-75251 Paris Cedex 05, France

The active form of human immunodeficiency virus type 1 protease (HIV-1 PR) is a homodimeric structure in which two subunits are linked through a two-stranded antiparallel β-sheet consisting of the N- and C-termini of each monomer. To inhibit the dimerization process or disrupt the dimeric interface leading to inactive enzyme, conformationally constrained "molecular tongs" have been designed and synthesized to interfere with one monomer end in a β-sheet fashion. These molecules are based on two peptidic strands attached to an aromatic scaffold. Inhibitions (submicromolar range) were obtained with molecular tongs containing tripeptidic or tetrapeptidic arms attached to a pyridinediol- or naphthalenediol-based scaffold ($K_{id} = 0.56$–4.5 μM at pH 4.7 and 30 °C). Kinetic studies are in agreement with an interface inhibition mechanism.

Introduction

HIV-1 protease (PR) has been studied and reviewed extensively, due to its importance as a therapeutic target to contend with AIDS. It plays a critical role in the maturation and infectivity of new viral particles.[1,2] Nevertheless, viral resistances to protease inhibitors administered alone or in combination with reverse transcriptase inhibitors have been described in vivo[3] suggesting that there is a need for structurally diverse antiproteases. All the protease inhibitors used in HIV-1 therapy (Saquinavir, Ritonavir, and Indinavir) interact with the active site preventing the binding of enzyme natural substrates. Another binding locus for HIV-1 PR inhibitors is the extended antiparallel β-sheet formed by the interdigitation of N-terminal (residues 1–4) and C-terminal (residues 96–99) β-strands of each monomer (Figure 1). Indeed, HIV-1 PR consists of two identical 99-residue monomers assembled into a C_2-symmetric structure, forming the active enzyme.[4–6] The interactions between the four termini contribute over 50% to the stabilizing force in the dimer. Blocking the assembly of the HIV-1 PR homodimer or disrupting the dimeric interface was suggested to be a novel means of inhibiting protease activity. The strategy of using interface peptides reproducing C- and N-terminal fragments to inhibit enzymatic activity has been applied successfully.[7–14] Zhang et al.[8] analyzed the kinetics of dimerization inhibition by the C-terminal tetrapeptide fragment and found it acted as a pure dimerization inhibi-

tor. This type of inhibition was confirmed by Schramm.[13] Babé et al. designed inhibitors containing two pentapeptide strands mimicking the N- and C-termini of a HIV-1 PR monomer connected with a three-glycine spacer.[10] Schramm et al. have proposed other inhibitors containing a five-glycine spacer to connect polypeptides, which were shown to be competitive site-directed inhibitors at high salt concentrations and mixed antidimer and competitive inhibitors at low salt concentrations.[13] More recently, Zutshi et al. synthesized interfacial peptides cross-linked with alkyl chains in order to reproduce the β-sheet structure with one HIV-1 PR monomer.[14] Their best inhibitor (IC$_{50}$ = 2 μM) was constructed with HN-PQITLW-OH and HN-STLNF-OH polypeptidic chains tethered with a C14 alkyl chain. The major drawback of these cross-linked inhibitors is related to their high conformational freedom which induces an unfavorable entropy term in the interaction energy of the inhibitor–HIV-1 PR monomer complex.

Our strategy has been directed toward the design of more rigid "molecular tongs" based on a conformationally constrained scaffold attached to two peptidic strands. The advantage of this strategy is that the two peptidic strands of the tongs could be originally suitably oriented by the scaffold allowing the formation of an antiparallel β-sheet with one HIV-1 PR monomer as illustrated in Figure 2, leading to entropic benefit. Three original rigid scaffolds have been chosen to link the two interface peptides. We explored the influence on the enzyme activity of (i) the nature of the scaffold and (ii) the length and sequence of the peptidic chains. Kinetic analyses

---

* To whom correspondence should be addressed. E-mail: sames.sicsic@cep.u-psud.fr.
§ Université de Paris-sud.
⊥ Universités de Paris VI et VII.

Figure 1. Stereoview of the antiparallel β-sheet formed by interdigitation of N- and C-terminal strands of each monomer of HIV-1 PR.

A

B

Tongs: $X_1 = X_2$ = peptide

Reference molecules: X_1 = peptide; X_2 = OMe

Figure 2. (A) Strategy of molecular tongs based on conformationally constrained scaffolds. (B) Structures of molecular tongs.

were performed in order to determine whether the designed molecules act as competitive or antidimer inhibitors.

Results and Discussion

The strategy of antidimer inhibition of HIV-1 PR was shown to be successful, more particularly by the use of interface peptides cross-linked with alkyl chains which were assumed to mimic the antiparallel β-sheet formed by N- and C-terminal residues of each monomer of HIV-1 PR.[13,14] Our strategy was based on the design of "molecular tongs" constrained by a rigid scaffold in order to orientate correctly two peptidic strands in an anti-

Scheme 1

parallel β-sheet structure and provide a suitable distance between them, close to the distance between the NH amide backbone of Pro 1 and Cys 95 of each monomer of dimeric HIV-1 PR (Figures 1 and 2). Using molecular modeling based on the crystallographic structure of HIV-1 PR, three constrained scaffolds were designed based on resorcinol, 2,6-pyridinediol, and 2,7-naphthalenediol on which carboxypropyl arms were bound (Figure 2). A distance of 10 Å between the two carbons of the carboxyl groups was reachable (Figure 2). The carboxypropyl arms also allowed some flexibility which may be necessary during the complexation process with one monomer of HIV-1 PR. For synthesis convenience, symmetrical tongs with two identical peptidic arms were synthesized using first the natural sequences TLNF and QITL (Figure 2).

Our strategy was to simplify these sequences in order to decrease the steric hindrance (TLVV versus TLNF) or the strand length (3 versus 4 amino acids) whereas the hydrophobic character was maintained (V instead of F or T). The sequence VLV was the ultimate simplification of TLV. To appreciate the usefulness of the two arms, molecules with only one peptidic arm were also prepared (Scheme 1). The scaffolds **1**, **3**, and **5** were synthesized using classical condensation reactions of ethyl 4-bromobutanoate with resorcinol, 2,6-pyridinediol, and 2,7-naphthalenediol, respectively. Partial hydrolysis of diester **5** with methanolic KOH gave rise to acid ester **6**, and total hydrolysis of compounds **1**, **3**, and **5** led to diacids **2**, **4**, and **7**, respectively. Finally, tongs **8**−**27** (Table 1) were obtained by condensation of the methyl esters of di-, tri-, or tetrapeptides on diacids **2**, **4**, and **7** using isobutyl chloroformate as the condensing agent.

Table 1. Inhibition of HIV-1 PR by Molecular Tongs at pH 4.7 and 30 °C

molecule	scaffold	X_1	X_2	analysis[a]	IC_{50}[b] (μM)
8	Res	QIOMe	QIOMe	$C_{38}H_{60}N_6O_{12} \cdot 2H_2O$[c]	ni[f]
9	Res	VLVOMe	VLVOMe	$C_{48}H_{80}N_6O_{12}$	ni
10	Res	TLVOH	TLVOH		ni
11	Pyr	TVOMe	TVOMe	$C_{33}H_{53}N_5O_{12} \cdot H_2O$	ni
12	Pyr	GLLOMe	GLLOMe	$C_{43}H_{71}N_7O_{12} \cdot H_2O$	16
					($K_{id} = 4.5\ \mu$M)
13	Pyr	TIVOMe	TIVOMe	$C_{45}H_{75}N_7O_{14} \cdot 2H_2O$	4.2
					($K_{id} = 1.4\ \mu$M)
14	Pyr	TLVOMe	TLVOMe	$C_{45}H_{75}N_7O_{14} \cdot 2H_2O$	I[g]
15	Pyr	VLVOMe	VLVOMe	$C_{47}H_{79}N_7O_{12}$	3
16	Pyr	TLVOH	TLVOH		34
17	Pyr	QITLOMe	QITLOMe	$C_{57}H_{95}N_{11}O_{18} \cdot H_2O$	ni
18	Pyr	TLNFOMe	TLNFOMe	$C_{61}H_{87}N_{11}O_{18} \cdot 3H_2O$	10
19	Naph	QIOMe	QIOME	$C_{42}H_{62}N_6O_{12}$d	ni
20	Naph	VLVOMe	VLVOMe	$C_{52}H_{82}N_6O_{12}, 2H_2O$	2
					($K_{id} = 0.56\ \mu$M)
21	Naph	TLVOMe	TLVOMe	$C_{50}H_{80}N_6O_{14}$	ni
22	Naph	TLVOBz	TLVOBz	$C_{62}H_{86}N_6O_{14} \cdot H_2O$	ni
23	Naph	TLVOH	TLVOH		10
24	Naph	TLYOMe	TLYOMe	$C_{58}H_{78}N_6O_{16} \cdot 2H_2O$[e]	ni
25	Naph	QITLOMe	QITLOMe	$C_{62}H_{98}N_{10}O_{18} \cdot 2H_2O$	ni
26	Naph	TLNFOMe	TLNFOMe	$C_{66}H_{90}N_{10}O_{18} \cdot 2H_2O$	4.4
					($K_{id} = 1\ \mu$M)
27	Naph	TLVVOMe	TLVVOMe	$C_{60}H_{96}N_8O_{16}$	ni
28	Naph	VLVOMe	OMe	$C_{36}H_{53}N_3O_9$	ni
29	Naph	TLVOMe	OMe	$C_{35}H_{51}N_3O_{10}$	I[h]
30	Naph	TLYOMe	OMe	$C_{39}H_{51}N_3O_{11}$	ni
31	Naph	QITLOMe	OMe	$C_{41}H_{61}N_5O_{12}$	ni
32	Naph	TLNFOMe	OMe	$C_{43}H_{57}N_5O_{12} \cdot 2H_2O$	I[i]
33	Naph	TLVVOMe	OMe	$C_{40}H_{58}N_4O_{11} \cdot H_2O$	10

[a] Analyses (C, H, N) are within the theoretical values $\pm$ 0.4% unless otherwise stated. [b] Standard errors are less than 15%. [c] N: calcd. 10.13; found, 9.35. [d] N: calcd. 9.97; found, 8.38. [e] H: calcd. 7.18; found, 7.63. [f] ni, no inhibition at the solubility limit. [g] 30% inhibition at 6.7 μM. [h] 30% inhibition at 4.5 μM. [i] 30% inhibition at 7 μM.

Table 2. ^{1}H NMR Chemical Shifts for the Peptides Branched after N-Deprotection to Scaffolds, Leading to Molecular Tongs

molecule	^{1}H NMR chemical shifts (NH, Hα, Hβ, Hγ)			
	AA_1	AA_2	AA_3	AA_4
BocQIOMe	5.55, 4.2, 1.95, 2.35	7.6, 4.45, 1.85, 1.15		
BocTVOMe	5.63, 4.0, 3.95, 0.95	7.2, 4.24, 1.93, 0.68		
BocTIVOMe	7.75, 4.18, 4.1, 1.05	7.82, 4.50, 2.50, 1.75	7.82, 4.48, 2.04	
ZGLLOMe	6.25, 3.85	7.45, 4.5, 1.55 (β, γ)	7.5, 4.6, 1.55 (β, γ)	
ZVLVOMe	5.52, 4.00, 2.08	6.55, 4.45, 1.55, 1.65	6.75, 4.45, 2.08	
ZTLVOMe	5.87, 4.29, 4.25, 1.14	6.97, 4.46, 1.57, 1.62	6.86, 4.51, 2.13	
BocTLYOMe	5.55, 4.15, 4.0, 1.08	6.95, 4.35, 1.5 (β, γ)	6.85, 4.75, 2.95	
BocQITLOMe	6.97, 3.9, 1.75/1.65, 2.05	7.9, 4.25, 1.8, 1.4	7.83, 4.2, 3.9, 1	7.67, 4.3, 1.3, 1.7
BocTLNFOMe	6.3, 3.9, 3.9, 1	7.84, 4.3, 1.4, 1.6	8.05, 4.5, 2.48/2.36	8.02, 4.4, 2.95
BocTLVVOMe	6.4, 3.9, 3.9, 0.95	7.55, 4.15, 1.55, 1.4	7.63, 4.2, 1.95	8.05, 4.35, 1.95

All the peptides were synthesized (Table 2) using isobutyl chloroformate, except for the condensation of XNGlnOH or XNAsnOH with the N-terminal part of other amino acids or peptides which were realized with DCC–HOBt method. Molecules **28**–**33** (Table 1), which possess only one peptidic arm branched on the naphthalenic scaffold, were obtained by the same condensation step from acid ester **6**.

Table 1 indicates the results of inhibition of HIV-1 PR by the synthesized molecules within their limit of solubility in test medium. No inhibition was observed with the resorcinol-based tongs **8**–**10**, whereas inhibitions were obtained with pyridinediol- and naphthalenediol-based tongs. These results allowed to estimate the influence of the scaffolds and of the length and sequence of the attached peptidic strands on the inhibition potency. Comparing the inhibitions of the pyridinediol-based tongs **15**, **16**, and **18** bearing VLV-OMe ($IC_{50} = 3\ \mu$M), TLV-OH ($IC_{50} = 34\ \mu$M), and TLNF-OMe ($IC_{50} = 10\ \mu$M), respectively, with the equivalent naphthalenediol-based tongs **20** ($IC_{50} = 2\ \mu$M), **23** ($IC_{50} = 10$
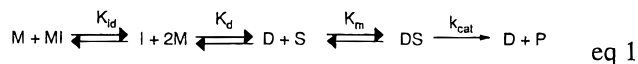
μM), and **26** ($IC_{50} = 4.4\ \mu$M), it can be deduced that the naphthalenediol-based scaffold was slightly better than the pyridinediol-based scaffold. In both series of tongs, the preferred sequences for inhibition could be classified as follows: VLV-OMe (**15**) $\sim$ TIV-OMe (**13**) > GLL-OMe (**12**) $\sim$ TLV-OMe (**14**) for the tripeptidic strands and VLV-OMe (**15**, **20**) > TLNF-OMe (**18**, **26**) if tripeptidic and tetrapeptidic strands are compared. Tongs with the peptidic sequences QI-OMe (**19**), TV-OMe (**11**), TLY-OMe (**24**), TLVV-OMe (**27**), and QITL-OMe (**17**, **25**) did not behave as inhibitors within their solubility limits. Generally, the inhibition was favored by the presence of two peptidic strands as exemplified by the comparison of **20** versus **28** and **26** versus **32**. The replacement of the ester end by the corresponding acid (**14** versus **16**) altered physicochemical properties, especially the solubility in buffer which was increased by a factor of 10, while a comparable enzymatic inhibitory potency was retained. Finally, it should be noted that pyridinediol- and naphthalenediol-based scaffolds without attached peptidic strands (**3** and **5**) were devoid of inhibitory
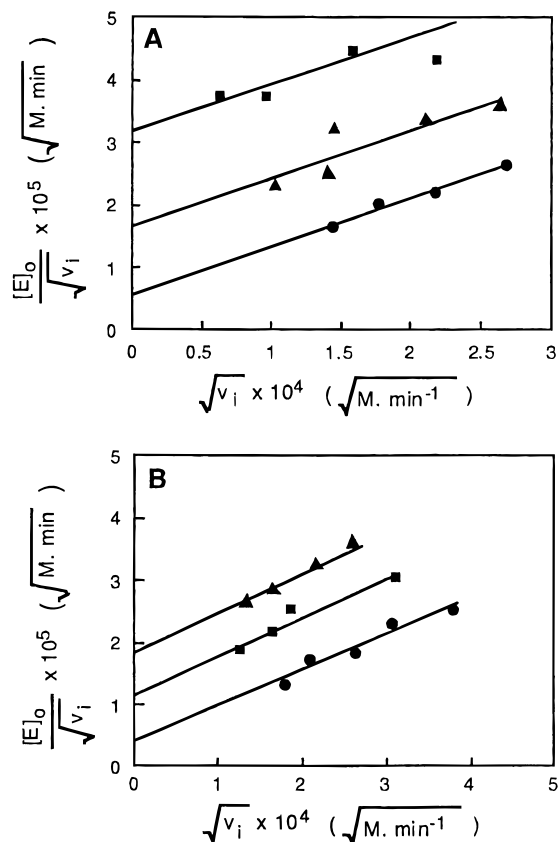
Figure 3. Plot of $[E]_0/\sqrt{v_i}$ versus $\sqrt{v_i}$ for hydrolysis of the fluorogenic substrate by HIV-1 PR at pH 4.7 and 30 °C in the absence (●) and presence of (A) 3 μM (▲), 6 μM (■), compound **13**; (B) 1 μM (■), 2 μM (▲) compound **20**. The enzyme concentrations were 2.37−9.47 nM, and the substrate concentration was 5.2 μM. The straight lines are curves calculated by regression fit to the data.

activity, as peptides alone, not attached to a rigid scaffold, excepted for TLV-OMe and TLVV-OMe which behaved as weak inhibitors (IC$_{50}$ > 30 μM).

To determine the type of inhibition which occurred with tongs, kinetic analyses of the inhibition process according to Zhang et al.[8] were performed with compounds **12**, **13**, **20**, and **26**. Plots of $[E]_0/\sqrt{v_i}$ versus $\sqrt{v_i}$ constructed for the four compounds studied gave straight lines with the same slope as without inhibitor, whatever the inhibitor concentration (Figure 3). These patterns were consistent with a dissociative inhibition described by the minimal kinetic scheme of eq 1, where D is the dimer, M is the monomer, S is the substrate, P is the product, and I is the inhibitor with $K_{id} = [M][I]/[MI]$, $K_d = [M]^2/[D]$, and K_m and k_{cat} are the kinetic parameters for the enzyme catalysis of substrate S hydrolysis. In our conditions the constant K_d was equal to 1.5 ± 0.25 nM. The values of K_{id} (equal to $[I]b_0/(b - b_0)$) were calculated from the intercepts in the presence (b) and absence (b_0) of inhibitor according to eq 2.

$$M + MI \underset{K_{id}}{\rightleftharpoons} I + 2M \underset{K_d}{\rightleftharpoons} D + S \underset{K_m}{\rightleftharpoons} DS \xrightarrow{k_{cat}} D + P \qquad \text{eq 1}$$

$$\frac{[E]_T}{\sqrt{v_i}} = \frac{K_m}{k_{cat}[S]_0}\sqrt{v_i} + \sqrt{\frac{K_m K_d}{4[S]_0 k_{cat}}}\left(1 + \frac{[I]_0}{K_{id}}\right) \qquad \text{eq 2}$$

These K_{id} values are indicated in Table 1; the best value
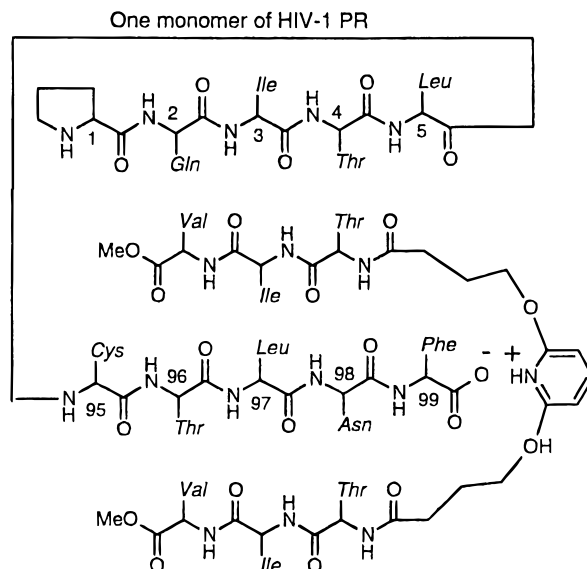
Figure 4. Schematic structure of the complex HIV-1 PR monomer/tong **13** showing potential ionic interaction between Phe-O$^-$ 99 of the protease and the protonated pyridine of compound **13**.

was obtained for compound **20** (K_{id} = 0.56 μM) which has two VLV-OMe strands attached to the naphthalenediol-based scaffold. It was verified that in the experimental conditions, the competitive inhibitor acetylpepstatin led to straight lines with the same intercept on the y axis.

These results may be discussed as follows: (i) The naphthalenediol- and pyridinediol-based scaffolds appear efficient to induce peptidic interface inhibition on HIV-1 PR, while the resorcinol-based scaffold appears inefficient. Indeed, compounds **9** and **10** were not inhibitors at concentrations for which equivalent naphthalenediol-based tongs **20** and **23** and pyridinediol-based tongs **15** and **16** inhibited HIV-1 PR. From a steric point of view, the necessary distance of 10 Å between the two peptidic strands of the tongs could be more easily reached by the naphthalenediol-based tongs than by the two other types of tongs. On the other hand, from an electronic point of view, only the pyridinediol-based tongs could form a favorable ionic interaction between the positively charged pyridine in the medium test and the negatively charged Phe-O$^-$ 99 of the C-end of HIV-1 PR monomer[15] (Figure 4). This argument is supported by the fact that scaffold **3**·*HCl* had a pK_A = 6.15 as measured potentiometrically. The assumption that steric effect and/or electronic effect is favorable for the tongs to induce inhibitory activity could explain why the resorcinol-based tongs were devoid of activity. (ii) The peptidic sequence TLNF-OMe reproducing the internal C-terminal strands of the antiparallel β-sheet of HIV-1 PR led to the active tongs **18** and **26**, while the peptidic sequence QITL-OMe reproducing the external N-terminus β-sheet strand led to the inactive tongs **17** and **25**. These results are consistent with those described in the literature where the best inhibitions were observed with interfacial peptides reproducing the C-terminal strand.[7−9,13] (iii) Surprisingly, the short peptidic sequence VLV-OMe appeared as the best sequence for inducing inhibitory potency (compounds **15** and **20**), although it did not reproduce the sequences involved in the natural antiparallel β-sheet of HIV-1 PR.

Our results could be compared with those of Zutshi et al.[14] who synthesized interfacial peptides cross-linked with polyalkyl chains. An IC_{50} value of 57 μM was obtained for the molecule displaying two identical interfacial peptides STLNF-OH cross-linked by the flexible spacer -(CO)-$(CH_2)_{12}$-(CO)-. With a rigid spacer (naphthalene) and a shorter peptidic sequence (TLNF-OMe, compound **26**), a better inhibitory potency was obtained (IC_{50} = 4.4 μM, K_{id} = 1 μM). The more potent inhibitor described by Zutshi et al. (IC_{50} = 2μM) was obtained with two different peptidic sequences reproducing the N- and C−termini of HIV-1 PR monomer (PQILW−OH and STLNF−OH, respectively, cross-linked with a 14-methylene spacer). With two identical and shorter peptidic strands (VLV-OMe, compound **20**), a comparable inhibitory efficiency was obtained (IC_{50} = 2 μM, K_{id} = 0.56 μM). The advantage of our tongs may be explained by the structural difference of the two types of spacers: aromatic-based spacers introduce a steric constraint which likely provides a positive entropic effect in contrast with the highly flexible spacers reported by Zutshi et al. A similar strategy based on a rigid scaffold was described by LaBrenz et al. in order to understand the energetics of β-sheet-based molecular recognition between a constrained peptide host and a linear peptide guest.[15] Finally, another advantage of constrained tongs resides in their symmetrical character allowing easy syntheses.

Conclusion

In this work, we have demonstrated the validity of the concept of constrained tongs built as two peptidic strands attached to a rigid naphthalenediol- or pyridinediol-based scaffold for inducing efficient antidimer inhibitions of the HIV-1 PR. This approach also shows that molecules with only tripeptidic strands which did not reproduce the N- and C-termini of HIV-1 PR monomer led to efficient inhibition. The best inhibitor is structurally simple and very easy to synthesize.

Experimental Section

HIV-1 protease was kindly supplied by H. J. Schramm, Max-Planck Institut für Biochemie (Martinsried, Germany). It was expressed using the plasmid pET9c-PR, and the isolation and purification procedure is described by Billich et al.[16] The stock solution (34 μM protease in 50 mM MES, pH 6.0, 1 mM EDTA, 1 mM DTT, 0.5 M NaCl, 5% v/v glycerol) was stored in small aliquots at −80 °C. The fluorogenic substrate DABCYL-S-Q-N-Y-P-I-V-Q-EDANS was purchased from Bachem. Reagents and solvents were from commercial sources. The fluorescence measurements were performed using a Jobin Yvon spectrofluorometer. NMR spectra were done on AC 200 Bruker and ARX 400 Bruker spectrometers. Elemental analyses were performed by the Service de microanalyse de la Faculté de Pharmacie. The pK_A measurements were performed in water using a Metrohm 632 pH apparatus equipped with a 614 impulsomat.

Enzymatic Assays. Enzymatic assays were performed in 100 mM sodium acetate, 1 mM EDTA, 1 M NaCl, pH 4.7, 3% DMSO (v/v). Inhibitors and the substrate were dissolved in DMSO before addition to the buffer. For the determination of IC_{50} values, 0.52 μL of a 3 mM solution of substrate (final concentration, 5.2 μM) was added to 8.5 μL of 4−10 different concentrations of inhibitors (final volume, 300 μL). The enzymatic reaction was initiated by the addition of enzyme (prediluted in buffer containing 1 mg/mL bovine serum albumin). The final enzyme concentration was 7.5 nM. The increase in fluorescence at 490 nm (λ_{exc} = 340 nm) was

monitored over a period of 5 min at 30 °C. For the more potent inhibitors the inhibition pathway was characterized using the kinetic analysis of Zhang et al.[8] The kinetic measurements were carried out with constant initial substrate concentration $[S]_0 \ll K_m$ (K_m = 103 μM)[17] using at least five different concentrations of enzyme (2.37−11.8 nM) for various concentrations of inhibitor.

Molecular Modeling. Molecular modeling was performed using a SGI Iris Indigo system (XS 4000) and the Sybyl 6.3 program from Tripos. Energy calculations were done using Tripos force field, Gesteiger−Marsilii charges, and a dielectric constant of 1. Crystallographic protease structure 8HVP downloaded from the Protein Data Bank was used. One monomer and the TLNF and QITL strands of the other monomer were retained. The tongs were built on the TLNF and QITL fragments in such a way that the minimization procedure of the obtained complexes converged easily (termination gradient of 0.5 kcal/mol·Å).

Chemistry. General Synthesis of Scaffolds. Example of Ethyl 4-((7-(4-Ethoxy-4-oxobutoxy)-2-naphthynyl)oxy)-butanoate (5). To a stirred solution of 2,7-dihydroxynaphthalene (10 g, 0.062 mol) and potassium carbonate (21.4 g, 0.155 mol) in DMF (200 mL) was added slowly ethyl 4-bromobutanoate (36.3 g, 0.186 mol). After 3 h solvent and excess reagent were evaporated, and the residue was dissolved in CH_2Cl_2 (100 mL). This solution was washed with water (2 × 50 mL), dried ($MgSO_4$), and evaporated. The resulting residue was chromatographed (silica gel, CH_2Cl_2) giving rise to **5** as an oily product (18.4 g, 75% yield): ^{1}H NMR ($CDCl_3$) δ 7.5 (d, 2H, J = 8 Hz), 6.94 (s, 2H), 6.90 (d, 2H, J = 8 Hz), 4.07 (q, 2H, J = 7 Hz), 4.06 (q, 2H, J = 7 Hz), 3.9 (t, 4H, J = 7 Hz), 2.5 (t, 4H, J = 7 Hz), 2.0 (m, 4H), 1.16 (t, 3H, J = 7 Hz), 1.15 (t, 3H, J = 7 Hz); ^{13}C NMR ($CDCl_3$) δ 173.6, 157.3, 135.8, 129, 124.3, 116.1, 106, 66.6, 60.4, 51.6, 30.8, 24.6. Anal. ($C_{22}H_{28}O_6$).

Ethyl 4-((3-(4-ethoxy-4-oxobutoxy)phenyl)oxy)butanoate (1): 85% yield; ^{1}H NMR ($CDCl_3$) δ 7.11 (t, 1H, J = 7 Hz), 6.43 (m, 3H), 4.11 (q, 4H, J = 7 Hz), 3.94 (t, 4H, J = 7 Hz), 2.41 (t, 4H, J = 7 Hz), 2.06 (m, 4H), 1.23 (t, 6H, J = 7 Hz); ^{13}C NMR ($CDCl_3$) δ 173, 159.9, 129.6, 106.6, 101.2, 66.5, 60.2, 30.6, 24.4, 14. Anal. ($C_{18}H_{26}O_6$).

Ethyl 4-((6-(4-ethoxy-4-oxobutoxy)-2-pyridyl)oxy)butanoate (3): 59% yield; ^{1}H NMR ($CDCl_3$) δ 7.29 (t, 1H, J = 8 Hz), 6.1 (d, 2H, J = 8 Hz), 4.14 (t, 4H, J = 6 Hz), 3.97 (q, 4H, J = 7 Hz), 2.32 (t, 4H, J = 7.5 Hz), 2.0−1.86 (m, 4H), 1.09 (t, 6H, J = 7 Hz); ^{13}C NMR ($CDCl_3$) δ 173.4, 162.6, 140.9, 101.4, 64.7, 60.3, 31.0, 24.6, 14.2. Anal. ($C_{17}H_{25}O_6 \cdot 1/4 H_2O$).

4-((7-(4-Methoxy-4-oxobutoxy)-2-naphthyl)oxy)butanoic Acid (6). A solution of diester **5** (1 g, 0.26 mmol) and NaOH (0.08 g, 2 mmol) in methanol (100 mL) was heated (50 °C) for 12 h and then evaporated and the residue put in water (50 mL). The aqueous solution was extracted with CH_2Cl_2 (2 × 50 mL) in order to remove the nonhydrolyzed diester, acidified (HCl, 10%), and extracted with CH_2Cl_2 (2 × 50 mL). This organic solution was washed with water, dried ($MgSO_4$), and evaporated giving **6** as a white cristalline product (0.3 g, 30% yield): mp 85 °C (petroleum ether−ether); ^{1}H NMR ($CDCl_3$) δ 7.63 (d, 2H, J = 7 Hz), 7.05−6.9 (m, 4H), 4.12 (t, 2H, J = 7 Hz), 4.08 (t, 2H, J = 7 Hz), 3.7 (s, 3H), 2.63 (t, 2H, J = 7 Hz), 2.55 (t, 2H, J = 7 Hz), 2.25−2.08 (m, 4H); ^{13}C NMR ($CDCl_3$) δ 179.5, 173.8, 157.3, 135.8, 129.1, 124.3, 116.2, 106.0, 66.6, 66.4, 51.7, 30.6, 24.6, 24.3. Anal. ($C_{19}H_{22}O_6$).

4-((7-(3-Carboxypropoxy)-2-naphthyl)oxy)butanoic Acid (7). A solution of ethanol (50 mL) containing **5** (6 g, 0.016 mmol) and 10% KOH (100 mL) was stirred at reflux for 4 h. Then the solution was poured in ice and extracted with CH_2Cl_2 (2 × 50 mL). The aqueous layer was acidified (HCl, 10%), and the precipitate was filtered and washed with water giving rise to a crystalline product. (5.84 g, 97% yield): mp 144 °C; ^{1}H NMR ($CDCl_3$) δ 7.75 (d, 2H, J = 7 Hz), 7.25 (d, 2H, J = 1.3 Hz), 7 (dd, 2H, J = 7 Hz, J = 1.3 Hz), 4.1 (t, 4H, J = 7 Hz), 2.5 (t, 4H, J = 7 Hz), 2 (m, 4H); ^{13}C NMR ($CDCl_3$) δ 174.1, 157, 136, 129, 123.8, 116, 106.2, 66.4, 30.2, 24.2. Anal. ($C_{18}H_{20}O_6$).

4-((3-(3-Carboxypropoxy)phenyl)oxy)butanoic acid (2): 95% yield; mp 170 °C; ^{1}H NMR (DMSO) δ 7.2−7.1 (m, 1H),

6.49−6.45 (m, 3H), 3.93 (t, 4H, $J = 6$ Hz), 2.34 (t, 4H, $J = 7$ Hz), 1.96−1.83 (m, 4H); ^{13}C MR (CDCl$_3$) δ 183.6. 169.2, 139.4, 116.2, 110.6, 76.0, 39.6, 33.8.

4-((6-(3-Carboxypropoxy)-2-pyridyl)oxy)butanoic acid (4): 88% yield; mp 92 °C (CH$_2$Cl$_2$−EtOH); ^{1}H NMR (CDCl$_3$) δ 7.45 (t, 1H, $J = 8$ Hz), 6.25 (d, 2H, $J = 8$ Hz), 4.33 (t, 4H, $J = 6$ Hz), 2.53 (t, 4H, $J = 7$. Hz), 2.15−2.02 (m, 4H); ^{13}C NMR (CDCl^3) δ 175.5, 163.9, 143, 102.5, 66.3, 31.6, 25.8. Anal. (C$_{13}$H$_{17}$NO$_6$·0.5H$_2$O).

General Synthesis of Tongs. Example of 13. In a solution of anhydrous DMF (20 mL) containing **4** (0.23 g, 0.83 mmol) and *N*-methylmorpholine (0.17 g, 1.6 mmol) maintained at −15 °C was added slowly isobutyl chloroformate (0.23 g, 1.6 mmol). The mixture was stirred for 2 h at −15 °C, and NH$_2$Thr-Ile-Val-OMe·HCl (0.8 g, 1.6 mmol) and *N*-methylmorpholine (0.17 g, 1.6 mmol) were added. The mixture was stirred for 15 h at room temperature. The resulting mixture was filtered, and the filtrate was evaporated to dryness. The crude solid was washed successively with warm water and methanol to give 0.7 g of **13** (90% yield).

References

(1) Kohl, N. E.; Emini, E. A.; Schleif, W. A.; Davis, L. J.; Heimbach, J. C.; Dixon, R. A. F.; Scolnick, E. M.; Sigal, I. S. Active Human Immunodeficiency Virus Protease is required for viral Infectivity. *Proc. Natl. Acad. Sci. U.S.A.* **1988**, *85*, 4686−4690.

(2) Peng, C.; Ho, B. K.; Chang, T. W.; Chang, N. T. Role of Human Immunodeficiency Virus Type 1-Specific Protease in Core Protein Maturation and Viral Infectivity. *J. Virol.* **1989**, *63*, 2550−2556.

(3) Roberts, N. A. Drug-resistance Patterns of Saquinavir and other HIV Protease Inhibitors. *AIDS* **1995**, *9*, 527−532.

(4) Navia, M. A.; Fitzgerald, P. M. D.; McKeever, B. M.; Leu, C. T.; Heimbach, J. C.; Heiber, W. K.; Sigal, I. S.; Darke, P. L.; Springer, J. P. Three-dimensional Structure of Aspartyl Protease from Human Immunodeficiency Virus HIV-1. *Nature* **1989**, *337*, 615.

(5) Wlodawer, A.; Miller, M.; Jaskolski, M.; Sathyanarayana, B. K.; Baldwin, E.; Weber, I. T.; Selk, L. M.; Clawson, L.; Schneider, J.; Kent, S. B. H. Conserved Folding in Retroviral Proteases: Crystal Structure of a Synthetic HIV-1 Protease. *Science* **1989**, *245*, 616−621.

(6) Lapatto, R.; Blundel, T.; Hemmings, A.; Overington, J.; Wilderspin, A.; Wood, S.; Merson, J. R.; Whittle, P. J.; Danley, D. E.; Geoghegan, K. F.; Hawrylik, S. J.; Lee, S. E.; Scheld, K. G.; Hobart, P. M. X-ray Analysis of HIV-1 Proteinase at 2.7 Å Resolution Confirms Structural Homology among Retroviral Enzymes. *Nature* **1989**, *342*, 299−302.

(7) Babé, L. M.; Pichuantes, S.; Craik, C. S. Inhibition of HIV Protease Activity by Heterodimer Formation. *Biochemistry* **1991**, *30*, 106−111.

(8) Zhang, Z.-Y.; Poorman, R. A.; Maggiora, L. L.; Heinrickson, R. L.; Kedzy, F. J. Dissociative Inhibition of Dimeric Enzymes. Kinetic Characterization of the Inhibition of HIV-1 Protease by its COOH-Terminal Tetrapeptide. *J. Biol. Chem.* **1991**, *266*, 15591−15594.

(9) Schramm, H. J.; Breipohl, G.; Hansen, J.; Henke, S.; Jaeger, E.; Meichsner, C.; Riess, G.; Ruppert, D.; Rücknagel, K.-P.; Schäfer, W.; Schramm, W. Inhibition of HIV-1 Protease by Short Peptides Derived from the Terminal Segments of the Protease. *Biochem. Biophys. Res. Commun.* **1992**, *184*, 980−985.

(10) Babé, L. M.; Rosé, J.; Craik, C. S. Synthetic Interface Peptides alter Dimeric Assembly of the HIV 1 and 2 Proteases. *Protein Sci.* **1992**, *1*, 1244−1253.

(11) Franciskovich, J.; Houseman, K.; Mueller, R.; Chmielewski, J. A Systematic Evaluation of the Inhibition of HIV-1 Protease by its C- and N-terminal Peptides. *BioMed. Chem. Lett.* **1993**, *3*, 765−768.

(12) Arnold, G. J.; Popinga, K.; Schramm, H. J.; Bell, M.; Thumfart, O.; Wenger, T.; Schramm, W. Inhibition of HIV-1 Protease by Bifunctional interface Peptides. In *Peptides 1994*; Maia, H. L. S., Ed.; ESCOM: Leiden, 1994; pp 345−346.

(13) Schramm, H. J.; Boetzel J.; Büttner, J.; Fritsche, E.; Görhing, W.; Jaeger, E.; König, S.; Thumfart, O.; Wenger, T.; Nagel, N. E.; Schramm, W. The Inhibition of Human Immunodeficiency virus proteases by Interface peptides. *Antiviral Res.* **1996**, *30*, 155−170.

(14) Zutshi, R.; Franciskovich, J.; Slultz, M.; Schweitzer, B.; Bishop, P.; Wilson, M.; Chmielewski, J. Targeting the Dimerization Interface of HIV-1 Protease: Inhibition with Cross-Linked Interfacial Peptides. *J. Am. Chem. Soc.* **1997**, *119*, 4841−4845.

(15) LaBrenz, S. R.; Kelly, J. W. Peptidomimetic Host that Binds a Peptide Guest Affording a β-Sheet Structure that subsequently self-assembles. A Simple Receptor Mimic. *J. Am. Chem. Soc.* **1995**, *117*, 1655−1656.

(16) Billich, A.; Hammerschmid, F.; Winkler, G. Purification, Assay and Kinetic Features of HIV-1 Proteinase. *Biol. Chem. Hoppe-Seyler* **1990**, *371*, 265−272.

(17) Matayoshi, E. D.; Wang, G. T.; Krafft, G. A.; Erickson, J. Novel Fluorogenic substrates for Assaying Retroviral Proteases by Resonance Energy transfer. *Science* **1990**, *247*, 954−958.